Available online at www.sciencedirect.com
SCIENCE DIRECT
ELSEVIER
International Journal of Mass Spectrometry 249–250 (2006) 403–411
International Journal of Mass Spectrometry
www.elsevier.com/locate/ijms

On the dissociation of the 2-pentanone ion studied by threshold photoelectron photoion coincidence spectroscopy

James P. Kercher [a], Bálint Sztáray [b], Tomas Baer [a,*]

[a] *Department of Chemistry, University of North Carolina, Chapel Hill, NC 27599-3290, United States*
[b] *The Department of General and Inorganic Chemistry, Eötvös Loránd University, Budapest, Hungary*

Received 21 October 2005; received in revised form 18 November 2005; accepted 21 November 2005
Available online 27 December 2005

Abstract

The photodissociation of 2-pentanone has been studied by threshold photoelectron photoion coincidence (TPEPICO) spectroscopy, in which ion time-of-flight (TOF) mass spectra are recorded as a function of the photon energy in the range of 9.6–12.2 eV. 2-Pentanone ions dissociate via four competitive channels: ethylene (C_2H_4) loss to produce the propen-2-ol ion, *n*-propyl ($^{\bullet}C_3H_7$) loss to produce the acetyl ion, and two parallel methyl ($^{\bullet}CH_3$) loss channels, producing the butanoyl ion at low energies and the but-3-en-2-ol ion at higher energies. The latter dissociates further via ethylene (C_2H_4) loss providing a second pathway to the acetyl ion. This final dissociation channel is observed experimentally by the appearance of an asymmetric ion peak in the time-of-flight (TOF) distribution at photon energies greater than 11.5 eV. The ion TOF distributions and breakdown diagram have been modeled in terms of the statistical RRKM theory for unimolecular reactions, yielding the 0 K dissociation onsets of 10.239 ± 0.015 eV for the butanoyl ion and 10.259 ± 0.019 eV for the propen-2-ol (acetone enolate) ion. By relating the measured onsets with other well established heats of formation, the 298 K heat of formation of the butanoyl and propen-2-ol ions were determined to be 586.9 ± 2.1 and 680.7 ± 1.8 kJ/mol, respectively. The acetone enolate ion is thus 37 kJ/mol more stable than the acetone ion, a value supported by G3B3, and CBS-QB3 calculations. The but-3-en-2-ol ion was found to lose ethylene to produce the acetyl ion without an energy barrier.

Keywords: 2-Pentanone; Propen-2-ol; Butanyol; TPEPICO; Enol

1. Introduction

The low energy dissociation channels of acetone [1,2] and butanone [3] ions have been well studied by photoionization and offer excellent routes for the determination of the acetyl and propionyl ion heats of formation. At low ion internal energies, these $RCOR'^{+}$ ions, where R and R′ can be any combination of $^{\bullet}CH_3$ and $^{\bullet}C_2H_5$, predominantly dissociate to produce carbonyl ions and neutral free radicals as described by Eqs. (1a) and (1b):

$$RCOR' + h\nu \rightarrow RCO^{+} + R', \quad E_0(1) \tag{1a}$$

$$RCOR' \rightarrow R + COR'^{+}, \quad E_0(2) \tag{1b}$$

These reactions have provided the major source of accurate heats of formation for the acetyl and propionyl ions through use of an energy equation such as:

$$E_0(1) = \Delta_f H^{\circ}[R'] + \Delta_f H^{\circ}[RCO^{+}] - \Delta_f H^{\circ}[RCOR'] \tag{2}$$

If two of the heats of formation are known, the third can be determined. The only complication is a minor side reaction in the case of acetone ions, which lose CH_4 [1,4–6]. In contrast, the 2-pentanone ion dissociates in a much more complex and interesting manner. Ethylene loss leads to the formation of the propen-2-ol (acetone enol) ion, a reaction first used by Holmes and Lossing [7] and then by Traeger [8] to obtain the heat of formation of the acetone enol ion. In addition, Murad and Inghram [9] used photoionization with deuterated samples to show that methyl loss can take place from both ends of the ion.

The problems associated with the extraction of thermochemical information from such disssociative photoionization onsets are well known. These include reactions with reverse activation barriers that lead to onsets higher than the thermochemical value. Another is the kinetic shift [10], which results from slow reaction rates that shift the observed onsets to higher energies. In the

* Corresponding author. Tel.: +1 919 962 1580; fax: +1 919 962 2388.
E-mail address: baer@unc.edu (T. Baer).

1387-3806/$ – see front matter © 2005 Elsevier B.V. All rights reserved.
doi:10.1016/j.ijms.2005.11.016

case of parallel reactions, the higher energy onset is invariable shifted to higher energy because of the competitive shift [10–12] with respect to the first dissociation channel. Experiments that simply measure the ion yield as a function of the ionizing energy, either by photoionization or by electron impact, are not sensitive to such effects and thus can lead to errors.

We have recently improved our threshold photoelectron photoion coincidence (TPEPICO) experiment by effectively suppressing the influence of hot electrons [1,3,13,14]. In combination with advances in the data analysis, which include incorporation of the thermal energy distribution and all of the various competitive and sequential dissociation channels, we can now model reactions of energy selected ions to very high energies.

In this study, we have collected new data on the 2-pentanone ion dissociation and have modeled the four parallel dissociation channels as well as a sequential reaction. Because much of the thermochemistry is fairly well established, this system provides an excellent test of our data and its analysis.

2. The TPEPICO experiment

The TPEPICO apparatus has been described in detail elsewhere [1,3,15], thus only a brief summary is given here. Room-temperature sample vapor is introduced into the ionization region through a small stainless steel capillary and ionized with vacuum ultraviolet (VUV) light from a hydrogen discharge lamp dispersed by a 1 m normal incidence monochromator with a resolution of 8 meV at a photon energy of 10.0 eV. The VUV wavelengths are calibrated by using the Lyman-α emission at 1215.67 Å, which is the most intense line in this spectrum. The ions and electrons are extracted in opposite directions with an electric field of 20 V/cm. Electrons pass through a second acceleration region where they are accelerated to a final energy of 74 eV. They then drift 13 cm along a field free drift region. The applied voltages are designed to velocity focus threshold electrons onto a 1.4 mm aperture at the end of the electron drift region, where a channeltron detects them. At the same time energetic electrons are focused to concentric rings around the central hole, the diameter of which is dependant on their initial perpendicular velocity component. Electrons hitting a 3 mm × 7 mm opening centered 5 mm away from the central hole are collected by a second channeltron and provide a measure of the hot electron signal. By subtracting a fraction of the coincidence spectrum obtained with the second channeltron from the TPEPICO spectrum, we obtain a TPEPICO spectrum free of 'hot' electron contamination.

The ions are accelerated to 100 eV in the first 5 cm long acceleration region and travel 40 cm in the first drift region. Ions are then reflected and travel through another 35 cm second drift region before being collected by a tandem multichannel plate ion detector. The electron and ion signals are used as start and stop pulses for measuring the ion time of flight (TOF). A complete TPEPICO TOF spectrum could be collected in 2–12 h. The TOF distributions, obtained at each photon energy, are used to obtain the fractional abundance of the precursor and the product ions (breakdown diagram).

If the dissociation is rapid, the fragment TOF peaks are symmetric. A reverse barrier in the dissociation channel, which is associated with significant translational energy release, appears as a peak broadening. On the other hand, a slow reaction, taking place on the time scale of microseconds, results in an asymmetric TOF peak because the ions are dissociating while accelerating in the 5 cm long acceleration region.

2-Pentanone was acquired from Aldrich Chemical Co. and used without further purification. No impurities were detected in the TPEPICO mass spectra.

3. Theoretical methodology

The data analysis, including RRKM rate constant calculations, requires knowledge of the vibrational frequencies of the starting molecule, the 2-pentanone ion, as well as the various transition states. These are best obtained from ab initio calculations, which were carried out at the DFT, G3B3 and CBS-QB3 levels of theory using the Gaussian 03 program suite [16] provided by the ITS Research computing facility at the University of North Carolina at Chapel Hill. The geometry and vibrational frequencies of all molecules studied were calculated using the Becke 3 parameter exchange functional [17], the correlation functional of Lee–Yang–Parr (B3LYP) [18] with the 6-311 + G** basis set. The harmonic frequencies of 2-pentanone, used in the calculation of the neutral internal energy distribution, are listed in Table 1. These frequencies were scaled as suggested by Andersson and Uvdal [19] who found that in B3LYP/6-311 + G** calculations, the low frequencies (below 100 cm^{-1}) should be scaled by 1.01, whereas the other vibrational frequencies should be scaled by 0.9679. The analysis of competitive dissociation pathways requires assumptions about the structure of the transition state. Those vibrational frequencies were also calculated at the B3LYP/6-311 + G** level of theory.

Finally, high level calculations at the G3B3 and CBS-QB3 level of theory were used to confirm the measured onsets for the known product ions, to provide insight into the products of each reaction, and to create isodesmic reactions which are used to support the derived thermochemistry.

4. Results

4.1. The TOF distributions and breakdown diagram

Time-of-flight (TOF) mass spectra were recorded in the energy range of 9.6–12.2 eV and selected TOF distributions are shown in Fig. 1. The solid lines through the experimental points are the simulated TOF profiles. At low energies, 10.289 eV, both the butanoyl ion (90.7 μs) and the propen-2-ol (82.0 μs) have slightly asymmetric peak shapes, which arise from parent ions that dissociate as they are being accelerated in the 5 cm acceleration region. The asymmetric peak shape indicates that the reaction rate is slow at the dissociation threshold, and that the rate constant is between 10^3 and 5×10^6 s^{-1}. It is in this range that the absolute rate constant can be extracted from the asymmetric TOF profile. The simulated TOF distributions given by the solid lines, and described later, match these metastable pro-

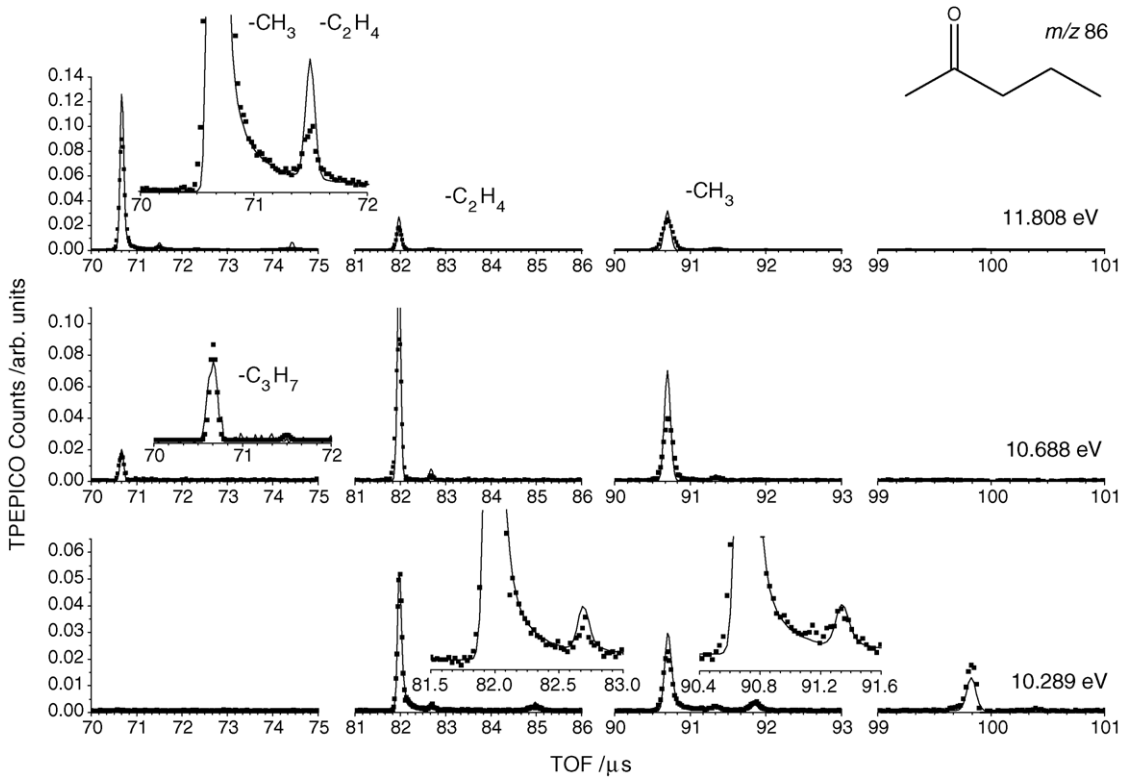

Fig. 1. Selected time-of-flight (TOF) distributions. At 10.289 eV, both the butanoyl ion (90.8 μs) and the propen-2-ol ion (82.0 μs) peaks are asymmetric. At 10.668 eV the acetyl ion peak has appeared at 70.7 μs as a symmetric peak. The butanoyl and propen-2-ol ions are now symmetric. At 11.808 eV, the acetyl ion (70.7 μs) is now asymmetric, indicating a sequential reaction pathway is energetically accessible.

files. There are also two small peaks at 91.9 and 85.0 μs, which result from dissociation of the parent ions in the drift region before the reflectron, which are also fitted.

The TOF spectrum at 10.688 eV in Fig. 1 shows the butanoyl and propen-2-ol ion peaks to be symmetric, indicating that the rate constant is now greater than $5 \times 10^6\ s^{-1}$. The acetyl ion peak, formed by the loss of the *n*-propyl radical, has also appeared at 70.7 μs. This peak is symmetric as well, because it is in competition with the other two fast channels. According to Murad and Ingrahm [9] the second methyl loss channel is now energetically accessible, but we are unable to distinguish the resulting ion from the butanoyl ion because they have the same mass. Because all the peaks are symmetric, no direct kinetic information is obtained at this ion internal energy.

The TOF distribution at 11.808 eV in Fig. 1 shows that the acetyl ion peak at 70.7 μs is now slightly asymmetric, a rather unexpected situation in that rate constants should increase with ion energy, rather than decrease! This indicates that a new dissociation channel has opened for the production of the acetyl ion. If this pathway were in competition with the lower energy channels, the rate constant would need to be greater than $5 \times 10^6\ s^{-1}$, and the peak would be symmetric. Because it is asymmetric, this dissociation channel cannot be in competition with the four lower energy pathways. We ascribe it instead to a sequential reaction. We propose that it results from the further or sequential dissociation of the ion produced from the second methyl loss channel, the but-3-en-2-ol ion, which can lose ethylene to produce the acetyl ion.

With the addition of a fifth dissociation pathway, the reactions, in order of increasing onset energy, along with the mass of the resulting ions are given below:

$$\text{2-pentanone} \rightarrow CH_3CH_2CH_2CO^+\ (71) + {}^{\bullet}CH_3 \quad (3a)$$

$$\rightarrow CH_3COH{=}CH_2^{\bullet+}\ (58) + C_2H_4 \quad (3b)$$

$$\rightarrow CH_3CO^+\ (43) + {}^{\bullet}C_3H_7 \quad (3c)$$

$$\rightarrow CH_3COHCHCH_2^+\ (71) + {}^{\bullet}CH_3 \quad (3d)$$

$$\hookrightarrow CH_3CO^+\ (43) + {}^{\bullet}CH_3 + C_2H_4 \quad (3e)$$

The most interesting point is that the five dissociation pathways yield three distinguishable mass peaks. There are two parallel methyl loss channels ((3a) and (3d)), resulting in the formation of two different ions, both of mass 71, and there are two different pathways for the production of the acetyl ion ((3c) and (3e)).

The breakdown diagram, given in Fig. 2, is a plot of the fractional ion abundance as a function of the photon energy. The points are the experimentally determined ion ratios, whereas the solid lines are simulated fits using the same parameters as employed in the TOF fitting. The dashed lines are the simulated curves that would be observed if the 2 methyl loss channels ((3a) and (3d)) were distinguishable and the dotted thin lines are for the 2 acetyl ion production channels ((3c) and (3e)). Summing the 2 methyl loss channels together and the 2 acetyl ion channels together produces the solid lines. The 0 K dissociation energies, E_0, obtained from the fits to the data are given in Table 2.

Table 1
Calculated vibrational frequencies at the B3LYP/6-311+G** level of theory

Species	Vibrational frequencies at B3LYP/6-311+G**
2-Pentanone[a]	48.5, 89.2, 97.1, 179.9, 250.5, 351.1, 410.2, 497.2, 616.6, 754.5, 851.5, 868.5, 938.8, 999.7, 1017.7, 1087.3, 1169.6, 1184.0, 1225.1, 1301.0, 1372.2, 1379.5, 1437.9, 1450.7, 1469.3, 1507.6, 1523.1, 1533.9, 1549.1, 1558.4, 1566.0, 1849.7, 3111.5, 3132.5, 3136.5, 3144.4, 3157.5, 3178.5, 3203.3, 3204.6, 3205.6, 3257.3
2-Pentanone$^+$	70.7, 138.3, 158.9, 219.1, 288.5, 315.9, 422.3, 485.8, 581.3, 682.8, 783.7, 869.7, 910.9, 924.0, 1003.7, 1030.5, 1078.6, 1107.2, 1130.4, 1207.3, 1256.0, 1326.8, 1377.0, 1392.2, 1430.3, 1449.2, 1481.9, 1491.2, 1491.3, 1513.3, 1529.5, 1735.3, 2921.2, 3050.5, 3122.4, 3152.0, 3174.3, 3180.9, 3225.9, 3233.7, 3234.7, 3300.6
But-3-en-2-ol$^+$	54.2, 128.0, 283.8, 430.0, 454.0, 584.7, 633.0, 712.7, 834.9, 991.6, 1007.2, 1043.9, 1078.5, 1093.8, 1166.3, 1330.4, 1366.5, 1386.2, 1439.4, 1456.6, 1493.6, 1555.6, 1655.0, 3023.4, 3075.6, 3132.7, 3156.3, 3199.5, 3253.8, 3721.3
$^{\bullet}CH_3$	537.0, 1402.4, 1402.4, 3103.2, 3282.9, 3283.0
TS (3a)	100[b], 185[b], 273[b], 356[b], 261.5, 215.5, 230.4, 259.0, 347.7, 420.3, 557.9, 757.7, 801.2, 880.1, 888.7, 938.8, 1031.2, 1124.4, 1160.9, 1275.6, 1283.6, 1369.0, 1405.6, 1455.9, 1459.9, 1461.8, 1479.0, 1548.7, 1550.0, 1558.9, 2417.7, 3127.0, 3158.8, 3180.6, 3184.2, 3204.8, 3221.5, 3240.5, 3245.0, 3385.4, 3389.2
TS (3b)	35[b], 46[b], 122[b], 153[b], 445.7, 466.6, 531.0, 575.2, 707.9, 784.5, 869.3, 897.2, 934.9, 1012.6, 1041.9, 1081.8, 1120.6, 1161.3, 1192.6, 1244.8, 1262.0, 1283.5, 1393.0, 1422.9, 1430.4, 1481.0, 1494.9, 1497.3, 1519.7, 1529.2, 1538.9, 1694.7, 3092.3, 3115.6, 3139.4, 3197.6, 3208.8, 3210.1, 3223.4, 3285.9, 3297.7
TS (3c)	65[b], 70[b], 83[b], 84[b], 96.7, 245.2, 254.5, 312.3, 355.1, 375.1, 761.5, 792.9, 915.4, 930.3, 935.3, 997.8, 1046.7, 1076.4, 1141.9, 1242.7, 1349.8, 1358.1, 1416.8, 1452.6, 1457.5, 1457.7, 1524.4, 1546.9, 1548.9, 1566.5, 2365.7, 3112.5, 3135.8, 3156.1, 3178.8, 3198.1, 3221.6, 3233.0, 3238.8, 3239.4, 3343.0
TS (3d)	40[b], 50[b], 90[b], 100[b], 261.5, 215.5, 230.4, 259.0, 347.7, 420.3, 557.9, 757.7, 801.2, 880.1, 888.7, 938.8, 1031.2, 1124.4, 1160.9, 1275.6, 1283.6, 1369.0, 1405.6, 1455.9, 1459.9, 1461.8, 1479.0, 1548.7, 1550.0, 1558.9, 2417.7, 3127.0, 3158.8, 3180.6, 3184.2, 3204.8, 3221.5, 3240.5, 3245.0, 3385.4, 3389.2
TS (3e)	260[b], 300[b], 400[b], 500[b], 574.7, 731.9, 848.4, 857.5, 910.7, 988.4, 1084.2, 1118.6, 1230.2, 1237.3, 1318.1, 1352.7, 1404.5, 1425.3, 1490.6, 1491.5, 1500.3, 2344.7, 3007.7, 3043.3, 3050.2, 3068.9, 3106.0, 3121.2, 3128.6

[a] Scaled as described in text.
[b] Denotes adjusted frequencies in the transition states.

4.2. Simulation of the experimental data

The solid line fits to the experimental data in Figs. 1 and 2 were obtained by taking into account the thermal energy distribution of 2-pentanone at the experimental temperature of 305 K as well as the photon and electron energy resolution of our instrument (15 meV). The ion internal energy distribution was calculated using the scaled 2-pentanone vibrational frequencies obtained from the ab initio calculations. The fit to the experiment was obtained by varying the assumed dissociation energies as well as the transition state vibrational frequencies. Varying the frequencies was necessary to model the slow dissociation rate of the methyl and ethylene loss reactions, as well as the sequential channel. It is often helpful to adjust the parameters in a sequential manner beginning with the first onset. Because the first two dissociation onsets are very close together, their fitting is not entirely independent so that they were fit together by adjusting the onset energy and the lowest four transition state vibrational frequencies for each reaction.

The extracted 0 K onsets for the butanoyl and propen-2-ol ions were determined to be 10.239 ± 0.015 and 10.259 ± 0.019 eV, respectively. The errors were determined by fixing the onsets at various energies in the vicinity of the optimum value and allowing the other parameters to vary. The error was then determined by noting at what energy a noticeable worsening of the fit was obtained. Because two reactions with very similar onset energies compete, the error limits are somewhat larger than ones obtained when only a single reaction dominates [15]. Both of these onsets were determined by previous experiments in which the fragment ion onset was measured as a function of the ionization energy for room temperature samples without taking into account the possible kinetic shift due to the slow reaction. We can convert these 298 K onsets to 0 K in an approximate manner by adding the rotational and vibrational energy to the 298 K onset. The Murad and Inghram [9] photoionization onset of 10.03 eV for the butanoyl onset converts to 10.207 eV at 0 K, which is some 32 meV lower than ours. Both Murad and Inghram using photoionization and Holmes and Lossing [7] using mono energetic electron ionization measured onsets for the higher energy propen-2-ol product, reporting converted 0 K onsets of 10.248 ± 0.08 and 10.257 ± 0.08 eV, respectively, which are both quite close to our more accurate value of 10.259 eV. Traeger [8] reported a 298 K onset of the propen-2-ol ion to be 10.03 ± 0.05 eV, which converts to 10.207 eV at 0 K. This value is lower than the other three by 41, 50 and 52 meV, respectively, though it is within the experimental error of each.

The acetyl ion production channel, associated with the loss of the *n*-propyl radical, is modeled by adjusting the E_0 and four

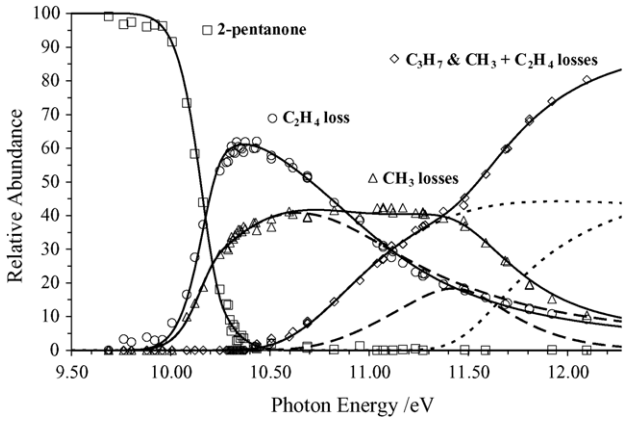

Fig. 2. The breakdown curve of 2-pentanone. The open points are the experimentally determined ion ratios, the dashed lines are the simulated methyl loss abundances, the dotted lines are the simulated acetyl ion abundances. Adding the dashed lines together and the dotted lines together produces the solid fit.

Table 2
Experimental and calculated dissociation onsets

Reaction products	Exp. E_0	Lit. E_0	CBS-QB3 E_0
Butanoyl ion + $^{\bullet}CH_3$	10.239 ± 0.015	10.207[a,b]	10.18[c]
Propen-2-ol ion + C_2H_4	10.259 ± 0.019	10.248[a,b], 10.257[d,b], 10.207 ± .05[e]	10.24[c]
Acetyl ion + $^{\bullet}C_3H_7$	10.483 ± 0.025	10.52[f]	10.47[c]
TS to enol	10.540 ± 0.033	–	10.20[c]
Acetyl ion + $^{\bullet}CH_3 + C_2H_4$	11.482 ± 0.037	11.486[g]	11.42[c]

All values are given in eV.
[a] From Murad and Inghram [9].
[b] AE converted to 0 K using $AE_{298K} = E_0 - \langle E_{rot}\rangle - \langle E_{vib}\rangle$.
[c] Calculated E_0 at the CBS-QB3 level of theory.
[d] From Holmes and Lossing [7].
[e] Traeger [8].
[f] Fogleman et al. [1].
[g] Based on known thermochemistry of the products and neutral 2-pentanone at 0 K.

lowest frequencies of the transition state. Although this reaction is fast in the energy region where it is observed, it must compete with the two lower energy channels so that its transition state frequencies must be adjusted. That is, these two parameters are varied to fit the relative rate of the acetyl ion production with respect to the other two channels. How rapidly the acetyl ion production channel catches up with the two lower energy dissociation channels is a function of the transition state frequencies. The resulting onset for the acetyl ion is calculated to be 10.483 ± 0.025 eV. Because this is a higher energy dissociation channel, the acetyl ion signal does not show a sharp onset, but rather blends smoothly into the background noise. This is because at its onset, the acetyl ion rate is several orders of magnitude smaller than the combined rates of the first two channels. Our fitting program takes all of this into account.

The second methyl loss channel associated with the methyl group on the long hydrocarbon chain is more complicated. Its only manifestation is in the breakdown diagram in which the flat topped profile from 10.5 to 11.4 eV suggests two processes. In fact, it was impossible to fit this profile by assuming a single methyl loss reaction. Because the onset of this ion was obscured by the lower energy butanoyl ion, the range of energies that provided a reasonable fit is wider. The E_0 and four lowest transition state frequencies were adjusted until the best fit over the entire energy range of the breakdown diagram was achieved, yielding an onset of 10.540 ± 0.033 eV. Although there are several adjustable parameters, the degree to which these parameters can be varied to reproduce a good fit over the entire energy range of the breakdown diagram is limited because there are three other competing channels, two of which are associated with asymmetric TOF distributions that yield direct kinetic information. That is, the amount of experimental information provides severe restraints on the range of the parameters. Based on ab initio calculations, we conclude that the ion produced in this reaction is the but-3-en-2-ol ion, rather than the higher energy ketone (but-3-en-2-one). The mechanism is discussed further in the next section.

As previously pointed out, the appearance of the slow acetyl ion reaction at higher energies must be attributed to a reaction that does not compete with the lower energy reactions. This new channel is also evident in the breakdown diagram in which the acetyl ion yield increases at 11.4 eV, rather than leveling off as would be expected for a single source reaction. This increase in the acetyl ion abundance is at the expense of the methyl loss channel. It is for this reason that we conclude that the but-3-en-2-ol ion (3d) further dissociates to the acetyl ion. The acetyl ion production rate is dependent on the energy partitioning between the but-3-en-2-ol ion and the neutral methyl ligand. Therefore the modeling requires knowledge of the ion and neutral structures as well as their vibrational frequencies. If reaction (3e) were fast, the only adjustable parameter would be E_0, and the shape of the breakdown diagram would be governed solely by the energy partitioning in reaction (3d), which has no adjustable parameters [14]. Because the reaction is slow, the transition state frequencies are also adjusted. This is done to fit the measured reaction rate as observed in the TOF distributions. The onset for the acetyl ion from the sequential reaction is 11.482 ± 0.037 eV. Because the final products (acetyl ion + $^{\bullet}CH_3 + C_2H_4$) have well established heats of formation shown in Table 3, we can calculate this onset to be 11.489 eV, an energy that agrees perfectly with the best fit to the data.

5. Theoretical results for the product ion identification

All reaction products were calculated at various levels of theory. Fig. 3 shows the potential energy diagram and compares the experimental dissociation onsets (dotted lines) and the calculated onsets (solid) at the CBS-QB3 level of theory. The transition state is calculated at the B3LYP/6-311+G** level of theory. The measured and calculated onsets (Table 2) for the butanoyl ion, propen-2-ol ion and acetyl ion agree very nicely, differing by 5.3, 1.8 and 0.9 kJ/mol, respectively. In addition, the sequential reaction for the formation of the acetyl ion agrees with the calculated value to within 5.8 kJ/mol. The only true disagreement is the fourth onset (3d), which does not agree with either the calculated but-3-en-2-one onset (too low by 50 kJ/mol) or the calculated but-3-en-2-ol onset (too high by 40 kJ/mol). The only reasonable explanation, confirmed by DFT calculations, is that the measured onset is associated with the transition state for the isomerization of the ketone to its enol structure. The QST3 method using B3LYP/6-311+G** was used to find the transition state, and the resulting energy differs from the measured onset

Table 3
Ancillary thermochemical values

Species	$\Delta_f H^\circ_{0\,K}$	$\Delta_f H^\circ_{298\,K}$	$H_{298\,K} - H_{o\,K}$ [a]
2-Pentanone	-230.2 ± 1.1 [a]	-258.8 ± 1.0 [b]	23.3
$^\bullet CH_3$	150.3 ± 0.4 [c]	147.1 ± 0.4 [d]	10.5
CH_4	-66.8 [a]	-74.4 [b]	9.99
C_2H_4	61.05 ± 0.4 [a]	52.5 ± 0.4 [b]	10.5
C_2H_6	-68.0 ± 0.4 [a]	-83.8 ± 0.4 [b]	11.7
CH_3CO^+	666.7 [e]	659.4 [e]	11.8
C_3H_6	35.7 ± 0.8 [a]	20.0 ± 0.8 [b]	15.7
$^\bullet C_3H_7$	118.0 [a]	100.2 [f]	15.5
C_3H_8	-82.2 ± 0.5 [a]	-104.7 ± 0.5 [b]	14.5
CH_3COCH_3	-202.2 ± 0.6 [a]	-218.5 ± 0.6 [g]	16.6
CH_3OH^+	846.0 [h]	856.9 [h]	11.5
CH_3NH_2	-8.3 ± 0.5 [a]	-23.0 ± 0.5 [b]	11.5
$C_3H_7NH_2$	-42.2 ± 0.4 [a]	-70.2 ± 0.4 [b]	17.6

All values given in kJ/mol.
[a] Converted using calculated vibrational frequencies from Table 1.
[b] Pedley [22].
[c] Determined from the $\Delta_f H^\circ_{0\,K}[CH_3^+]$ from Weitzel et al. [31] and the IE[$^\bullet CH_3$] from Blush et al. [32].
[d] Weitzel et al. [31].
[e] Fogelman et al. [1].
[f] Tsang [36].
[g] From Wiberg et al. [33].
[h] From $\Delta_f H^\circ_{0\,K}[CH_3OH]$ from Pedley [34] and IE[CH_3OH] from Tao et al. [35].

by about 13 kJ/mol. Therefore, the measured onset must be associated with the isomerization barrier to the enol form of the ion. The lowest energy dissociation pathway from the enol is for the production of the but-3-en-2-ol ion ($CH_3COHCH{=}CH_2^+$), which lies approximately 90 kJ/mol below the but-3-en-2-one ion onset. It is the but-3-en-2-ol ion that dissociates further via an ethylene loss channel to produce the acetyl ion.

6. Experimental and theoretical thermochemistry

The 298 K heat of formation of neutral 2-pentanone was determined by Harrop et al. [20] and is listed in Cox and Pilcher's thermochemical compilation [21] as -259.1 ± 1.1 kJ/mol. This has been updated in Pedley's [22] recent compilation to -258.8 ± 1.0 kJ/mol. Because the determination of the thermochemistry hinges on the 2-pentanone heat of formation, we have used four homodesmotic reactions to verify the neutral 2-pentanone heat of formation. These reactions are summarized below:

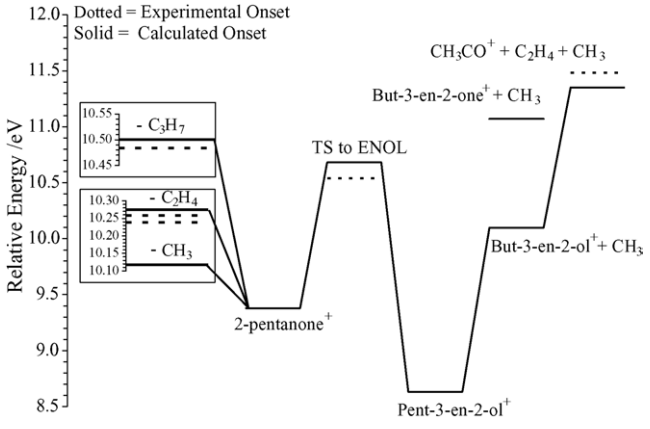

Fig. 3. Comparison of the experimental and calculated onset energies for all five dissociation pathways. All stable species were calculated at the CBS-QB3 level of theory from the B3LYP/6-311+G** optimized structure. The transition state was calculated at the B3LYP/6-311+G** level of theory.

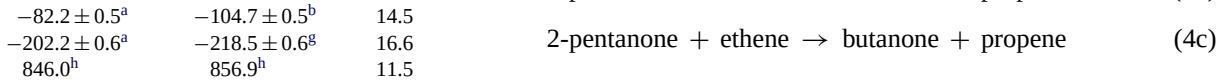

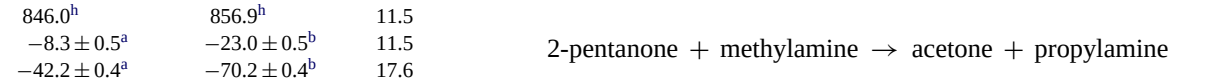

The reaction energy for these four reactions were calculated at the G3B3 and CBS-QB3 levels of theory, and the 2-pentanone heat of formation obtained by using well known heats of formation of all the other species (Table 3). The results of these calculations yielded an average $\Delta_f H^\circ_0$[2-pentanone] = -230.6 ± 0.3 kJ/mol, which compares nicely with the experimental heat of formation of -230.2 ± 1.1 kJ/mol.

The onset energies for the various fragment ions are related to the heats of formation of the reactants and products. The least well established heats of formation are those of the butanoyl ion and the propen-2-ol ion (enol of acetone). Because these are the first two onsets, and the associated neutral species ($^\bullet CH_3$, C_2H_4, and 2-pentanone) are well known, we can use our analysis to establish accurate heats of formation for these two ions. For instance, the onset for the butanoyl ion (first $^\bullet CH_3$ loss reaction) at 10.239 ± 0.015 eV is related to reactant and product heats of formation as shown in Eq. (6).

$$E_0 = \Delta_f H^\circ_{0\,K}[\text{butanoyl ion}] + \Delta_f H^\circ_{0\,K}[^\bullet CH_3] - \Delta_f H^\circ_{0\,K}[\text{2-pentanone}] \quad (6)$$

This yields a butanoyl ion 0 K heat of formation of 606.7 ± 2.1 kJ/mol, which can be converted to a 298K value, using Eq. (7),

$$\Delta_f H^\circ_{298\,K} = \Delta_f H^\circ_{0\,K} - \sum (H^\circ_{298\,K} - H^\circ_{0\,K})_{\text{elements}} + \sum (H^\circ_{298\,K} - H^\circ_{0\,K})_{\text{molecule}} \quad (7)$$

in which the $(H^\circ_{298\,K} - H^\circ_{0\,K})_{\text{elements}}$ values are taken from Wagman et al. [23] and the $(H^\circ_{298\,K} - H^\circ_{0\,K})_{\text{molecule}}$ values are calculated using the vibrational frequencies in Table 1. This conversion results in a 298 K heat of formation of 586.9 ± 2.1 kJ/mol.

Similarly, the measured onset for reaction (3b), along with the ancillary heats of formation of 2-pentanone and ethylene in Table 3, yields a 0 K heat of formation for the propen-2-ol ion of 697.9 ± 1.8 kJ/mol, which converts to 680.7 kJ/mol at 298 K. It is interesting that Holmes and Lossing [7], although obtaining the same measured onset as we do here, reported a $\Delta_f H^\circ_{298\,K}$[propen-2-ol ion] to be 661 kJ/mol, which is some 20 kJ/mol lower than our value. This result, which is listed in

Table 4
Thermochemistry of the reaction products

Species	Exp. $\Delta_f H^\circ_{0\,K}$	Exp. $\Delta_f H^\circ_{298\,K}$	Lit. $\Delta_f H^\circ_{298\,K}$	$H_{298\,K} - H_{o\,K}$
Butanoyl ion	606.7 ± 2.1	586.9 ± 2.1	584.2[a]	18.4[b]
Propen-2-ol ion	697.9 ± 1.8	680.7 ± 1.8	681.2[a], 681.6[c]	16.3[b]

All values given in kJ/mol.
[a] From Murad and Inghram [9].
[b] Calculated using vibrational frequencies at the DFT B3LYP/6-311+G** level of theory.
[c] From Holmes and Lossing [7] using updated conversion to E_0.

the NIST [24] website as the heat of formation of the acetone enol ion, is obtained by using their phenomenological 298 K onset along with 298 K heats of formation for the 2-pentanone and ethylene without taking into account the proper treatment of such onsets [25] (a commonly committed error in the early 1980s). This was noted by Turecek and Crammer [26], who applied the correction to the original Holmes and Lossing value, resulting in a 298 K heat of formation of 684 kJ/mol. Turecek and Cramer used a G2(MP2) ab initio study to obtain a $\Delta_f H^\circ_{298\,K}$[propen-2-ol ion] of 677 kJ/mol. Traeger [8] also determined the $\Delta_f H^\circ_{298\,K}$[propen-2-ol ion] from the dissociative photoionization of a series of methyl ketones, including 2-pentanone. The resulting $\Delta_f H^\circ_{298\,K}$[propen-2-ol ion] from 2-pentanone was determined to be 676.9 kJ/mol, while the mean average of the four measurements is 676.6 ± 0.7 kJ/mol.

Because the experimentally measured propen-2-ol ion heats of formation vary by ∼8 kJ/mol, we have determined it using high level calculations with the isodesmic reaction:

$$\text{propen-2-ol}^+ + \text{methane} \rightarrow \text{methanol}^+ + \text{propene} \quad (8)$$

With the well established heats of formation of methane, propene and the methanol ion (see Table 3) the calculated 0 K G3B3 and CBS-QB3 enol ion heats of formation were 698.8 and 698.4 kJ/mol, respectively. At 298 K, these values of 682.3 and 681.8 kJ/mol, respectively, agree extremely well with our measured value of 680.7 ± 1.8 kJ/mol for the $\Delta_f H^\circ_{298\,K}$[propen-2-ol ion]. Using other alcohols in the isodesmic reaction can lead to error, because the adiabatic ionization energies of most the other alcohols are not well established because Franck–Condon factors do not favor the adiabatic transition. This is because of the large geometry change between the neutral and ion ground states.

Trikoupis et al. [27] recently calculated the acetone enol ion to be 42.2 kJ/mol more stable than the acetone radical cation using the CBS-Q/DZP level of theory. This supports the B3LYP/cc-pVTZ level theory calculation of Nummela and Carpenter [6], who reported an energy difference of 42 kJ/mol. If we assume an acetone ion heat of formation at 0 K of 734.5 kJ/mol, obtained from the ionization energy reported by Fogleman et al. [1] and the heat of formation of neutral acetone from Wiberg et al. [28], the Nummela and Carpenter enol ion heat of formation (after conversion to 298 K) is 675.8 kJ/mol, which is 6 kJ/mol lower than our measurement, and is in much better agreement with the value of 676.6 reported by Traeger (Table 4).

7. Discussion

On the basis of our measured methyl loss onset, which confirms the Murad and Inghram [9] measurement, the heat of formation of the butanoyl ion is now well established. This ion heat of formation will be used in our current TPEPICO study of 2,3-hexanedione. The 2,3-hexanedione ion dissociates to produce the butanoyl ion and acetyl radical at low energies, followed by the acetyl ion and butanoyl radical at higher energies, as shown below:

$$CH_3COCOCH_2CH_2CH_3 \rightarrow CH_3CO + COCH_2HC_2CH_3^+, \quad E_0(1) \quad (9a)$$

$$CH_3COCOCH_2CH_2CH_3 \rightarrow CH_3CO^+ + COCH_2CH_2CH_3, \quad E_0(2) \quad (9b)$$

$E_0(1)$ can be used with acetyl radical and butanoyl ion heat of formation to determine the 2,3-hexanedione neutral heat of formation, which can then be applied with $E_0(2)$ and the acetyl ion heat of formation to yield the butanoyl radical heat of formation. Because the 2,3-hexanedione ion dissociation is made complicated by a sequential reaction of the butanoyl ion to produce the acetyl ion, a full analysis of the dissociation dynamics and onset energies will be reported in a subsequent paper.

The propen-2-ol ion heat of formation derived from the 2-pentanone ion dissociative ionization onset has now been measured by Murad and Inghram [9], Holmes and Lossing [7], Traeger [8], and ourselves. Three of the experiments agree on the higher value, and Traeger's onset is lower by about 50 meV. The competition between the two dissociation channels and the fact that the onsets occur in a Franck–Condon gap present some problems in establishing a reliable onset. Under these circumstances, our TPEPICO experiment is ideally designed to establish an accurate onset so that we favor our value of 680.7 ± 1.8 kJ/mol for the $\Delta_f H^\circ_{298\,K}$[propen-2-ol ion]. The various calculations also disagree. Turecek and Cramer [26] and Numella and Carpenter [6] obtain values that are about 5 kJ/mol lower, around ∼677 kJ/mol. As with the discrepancies among the experimental values, we favor our own value, which is carried out at a higher level than the others and also agrees with our experimental finding.

An interesting finding in this study is the high energy acetyl ion onset energy, which proceeds via a sequential loss of the methyl radical followed by an ethylene loss step. The fact that

this onset is identical to the thermochemically expected one indicates that there is no barrier to this ethylene reaction. However, on energetic grounds, the acetyl ion could equally well go via an ethylene loss from 2-pentanone ion to form the acetone enol ion, followed by a methyl loss. Yet, the breakdown diagram shows that the second onset for the acetyl ion comes at the expense of the methyl loss channel (see breakdown diagram in Fig. 2). By contrast, the ethylene loss channel in Fig. 2 follows the pattern expected for simple reaction, with no evidence for a sequential loss of the methyl radical.

The fact that the enol ion of acetone does not readily lose a methyl radical is well known. The only way for the enol to dissociate to the acetyl ion is by isomerizing to the keto form of acetone [29]. Lifshitz was one of the first to point out that this involves a barrier [30]. This conclusion was based on a non-statistical energy distribution caused by a 150 kJ/mol reverse barrier. More recent calculations of Numella and Capenter [6] indicate an even higher barrier of 159 kJ/mol. The barrier is a result of the difficult H atom transfer via a 4-center transition state.

The interesting question that remains is: why is there no barrier in the acetyl ion formation from the but-3-en-2-ol ion? This enol must also transfer its H atom prior to ethylene loss. A major difference between this ion and the acetone enol ion is that the double bond is one carbon atom removed from the carbonyl C atom [C–C(OH)–C=C] rather than adjacent to the carbonyl group in the acetone enol ion.

8. Conclusions

The dissociation of 2-pentanone ions is both interesting and complex. The parent ion can undergo ethylene loss, *n*-propyl loss and two competing methyl loss channels. The higher energy methyl loss channel involves isomerization into an enol well. In addition, it dissociates further via ethylene loss. The breakdown diagram and TOF distributions have been modeled in terms of the RRKM framework and the 0 K dissociation onsets have been determined. Quantum chemical calculations have been used widely to support the measured onsets and derived thermochemistry and to identify the product ion structure.

We report on the heats of formation of the butanoyl and propen-2-ol ions. We have shown that the measured onsets for the higher energy dissociation channels can be determined accurately. In addition to the derived thermochemistry, the photodissociation of the 2-pentanone ion illustrates the clever ways in which these ions can dissociate, via rearrangements and enol wells. Our TPEPICO data have illuminated the hidden dissociation channels, which if unaccounted for can lead to large errors in the determined onsets which propagate to the derived thermochemistry. Even in this complicated reaction, the statistical theory within the RRKM framework can be applied successfully.

Acknowledgements

We gratefully thank the Department of Energy and the International Office of the National Science Foundation for the support of this work. One of the authors (JPK) wishes to thank the Center for International Studies at the University of North Carolina for their gracious support to allow much of this work to be done in Budapest, Hungary.

References

[1] E.A. Fogleman, H. Koizumi, J.P. Kercher, B. Sztáray, T. Baer, J. Phys. Chem. A 108 (2004) 5288.
[2] J.C. Traeger, R.G. McLoughlin, A.J.C. Nicholson, J. Am. Chem. Soc. 104 (1982) 5318.
[3] J.P. Kercher, E.A. Fogleman, H. Koizumi, B. Sztáray, T. Baer, J. Phys. Chem. A 109 (2005) 939.
[4] N. Heinrich, F. Louage, C. Lifshitz, H. Schwarz, J. Am. Chem. Soc. 110 (1988) 8183.
[5] W.M. Trott, N.C. Blais, E.A. Walters, J. Chem. Phys. 69 (1978) 3150.
[6] J.A. Nummela, B.K. Carpenter, J. Am. Chem. Soc. 124 (2002) 8512.
[7] J.L. Holmes, F.P. Lossing, J. Am. Chem. Soc. 102 (1980) 1591.
[8] J.C. Traeger, Int. J. Mass Spectrom. 210/211 (2001) 181.
[9] E. Murad, M.G. Inghram, J. Chem. Phys. 40 (1964) 3263.
[10] W.A. Chupka, J. Chem. Phys. 30 (1959) 191.
[11] F.S. Huang, R.C. Dunbar, J. Am. Chem. Soc. 112 (1990) 8167.
[12] C. Lifshitz, Mass Spectrom. Rev. 1 (1982) 309.
[13] B. Sztáray, T. Baer, Rev. Sci. Instrum. 74 (2003) 3763.
[14] T. Baer, B. Sztáray, J.P. Kercher, A.F. Lago, A. Bodi, C. Scull, D. Palathinkal, Phys. Chem. Chem. Phys. 7 (2005) 1507.
[15] A.F. Lago, J.P. Kercher, A. Bodi, B. Sztáray, B.E. Miller, D. Wurzelmann, T. Baer, J. Phys. Chem. A 109 (2005) 1802.
[16] M.J. Frisch, G.W. Trucks, H.B. Schlegel, G.E. Scuseria, M.A. Robb, J.R. Cheeseman, J.A. Montgomery, T. Vreven, K.N. Kudin, J.C. Burant, J.M. Millam, S.S. Iyengar, J. Tomasi, V. Barone, B. Mennucci, M. Cossi, G. Scalmani, N. Rega, G.A. Petersson, H. Nakatsuji, M. Hada, M. Ehara, K. Toyota, R. Fukuda, J. Hasegawa, M. Ishida, T. Nakajima, Y. Honda, O. Kitao, H. Nakai, M. Klene, X. Li, J.E. Knox, H.P. Hratchian, J.B. Cross, C. Adamo, J. Jaramillo, R. Gomperts, F. Stratmann, O. Yazyev, A.J. Austin, R. Cammi, C. Pomelli, J.W. Ochterski, P.Y. Ayala, K. Morokuma, G.A. Voth, P. Salvador, J.J. Dannenberg, V.G. Zakrzewski, S. Dapprich, A.D. Daniels, M.C. Strain, Ö. Farkas, D.K. Malick, A.D. Rabuck, K. Raghavachari, J.B. Foresman, J.V. Ortiz, Q. Cui, A.G. Baboul, S. Clifford, J. Cioslowski, B.B. Stefanov, G. Liu, A. Liashenko, P. Piskorz, I. Komáromi, R.L. Martin, D.J. Fox, T. Keith, M.A. Al-Laham, C.Y. Peng, A. Nanayakkara, M. Challacombe, P.M.W. Gill, B. Johnson, W. Chen, M.W. Wong, C. Gonzalez, J.A. Pople, Gaussian 03, Revision C. 02, Gaussian, Inc., Pittsburgh PA, 2004 (Ref Type: Computer Program).
[17] A.D. Becke, J. Chem. Phys. 97 (1992) 9173.
[18] C. Lee, W. Yang, R.G. Parr, Phys. Rev. B37 (1988) 785.
[19] M.P. Andersson, P. Uvdal, J. Phys. Chem. A 109 (2005) 2937.
[20] D. Harrop, A.J. Head, G.B. Lexis, J. Chem. Therm. 2 (1970) 203.
[21] J.D. Cox, G. Pilcher, Thermochemistry of Organic and Organometallic Compounds, Academic Press, London, 1970.
[22] J.B. Pedley, Thermochemical Data and Structures of Organic Compounds, Thermodynamics Research Center, College Station, 1994.
[23] D.D. Wagman, W.H.E. Evans, V.B. Parker, R.H. Schum, I. Halow, S.M. Mailey, K.L. Churney, R.L. Nuttall, The NBS Tables of Chemical Thermodynamic Properties, J. Phys. Chem. Ref. Data, vol. 11, Suppl. 2, NSRDS, U.S. Government Printing Office, Washington, 1982.
[24] http://webbook.nist.gov/chemistry/om/.
[25] J.C. Traeger, R.G. McLoughlin, J. Am. Chem. Soc. 103 (1981) 3647.
[26] F. Turecek, C.J. Cramer, J. Am. Chem. Soc. 117 (1995) 12243.
[27] M.A. Trikoupis, P.C. Burgers, P.J.A. Ruttink, J.K. Terlouw, Int. J. Mass Spectrom. 217 (2005) 97.
[28] K.B. Wiberg, L.S. Crocker, K.M. Morgan, J. Am. Chem. Soc. 113 (1991) 3447.
[29] F.J. McLafferty, D.J. McAdoo, J.S. Smith, R. Kornfeld, J. Am. Chem. Soc. 93 (1971) 3720.
[30] C. Lifshitz, E. Tzidony, Int. J. Mass Spectrom. Ion. Proc. 39 (1981) 181.

[31] K.M. Weitzel, M. Malow, G.K. Jarvis, T. Baer, Y. Song, C.Y. Ng, J. Chem. Phys. 111 (1999) 8267.
[32] J.A. Blush, P. Chen, R.T. Wiedmann, M.G. White, J. Chem. Phys. 98 (1993) 3557.
[33] K.B. Wiberg, L.S. Crocker, K.M. Morgan, J. Am. Chem. Soc. 113 (1991) 3447.
[34] J.B. Pedley, Thermochemical Data and Structures of Organic Compounds, Thermodynamics Research Center, College Station, 1994.
[35] W. Tao, R.B. Klemm, F.L. Nesbitt, J.L. Stief, J. Phys. Chem. 96 (1992) 104.
[36] W. Tsang, Energetics of Organic Free Radicals, Chapman & Hall, London, 1996, pp. 22–58 (Chapter 2).